Hindawi
Advances in Materials Science and Engineering
Volume 2020, Article ID 6428032, 12 pages
https://doi.org/10.1155/2020/6428032

Research Article

An Experimental Study on the Ecological Support Model of Dentate Row Piles

Yousheng Deng, Zhihe Cheng, Mengzhen Cai, Yani Sun, and Chengpu Peng

School of Civil Engineering & Architecture, Xi'an University of Science and Technology, Xi'an, China

Correspondence should be addressed to Zhihe Cheng; 17204054005@stu.xust.edu.cn

Received 22 May 2019; Revised 1 September 2019; Accepted 6 January 2020; Published 22 January 2020

Academic Editor: Antonio Boccaccio

Bamboo is highly renewable and biodegradable with good short-term strength, which meets the requirement for temporal support structures in shallow foundation pits. Based on this, we conducted a laboratory model test on the dentate bamboo micropile support structure combined with environmentally friendly building materials and new type of piles, to explore the stress characteristics, stress change regularity, and the support effect of the system in soft soil foundation pits. The results show that the earth pressure on the pile sides above the excavation surface gradually decreases with an increase in the excavation depth. The bending deformation of the bamboo pile was also significant. The results also show that the earth pressure and the pile strain below the excavation surface change slightly during the excavation process. When the short sides of the foundation pit were loaded, the highest strain was recorded in the piles 4 and 11. A maximum strain of 358.93 $\mu\varepsilon$ was recorded, and the maximum displacement of the pile in the top part was obtained to be only 2.14 mm. The most subsidence of dentate pile obtained is only 1.88 mm, whereas that of the single-row pile is 2.35 mm. Compared to the traditional single-row pile, the dentate piles can effectively reduce the horizontal deformation as well as the surface subsidence effectively. They can also support more external lateral load, and hence maintain the foundation stability and give better support. The results provide a theoretical basis for ecological bamboo support technology and have great value to be promoted.

1. Introduction

Currently, steel and cement are used to form the main part of foundation-pit support structures in China. However, use of these materials for the structures involves high energy consumption and causes emission and pollution. Moreover, this type of support structures, usually temporary, is difficult to remove after the completion of the foundation construction. They are also costly, cumbersome to transport, and affects the construction period. Abandoning the structure in the soil not only causes pollution to the soil but also poses a threat to the construction of any nearby underground projects. The problem of underprevention or overprevention is also common in the traditional and the simple parallel single-row or double-row piles because of the complexity and specialty of soft soil. Meanwhile, most building materials are often steel bars and concretes. It is, therefore, necessary to create a new pile laying method, which would have high strength and positive support effects as well as be environmentally friendly. Bamboo has a short growth period, high yield, and superior short-term mechanical properties. As a renewable natural material, bamboo is widely used in engineering with the development of its processing technology and the concept of green development [1]. In Fujian and Shanghai, China, parts of the shallow foundation engineering in soft soil, which were supported with the preventive single-row or double-row bamboo piles or bamboo-soil-nailing-wall support structures, achieved great support as well as high economic value. In this study, a new laying method of piles is integrated with energy-saving building materials to investigate the stress mechanism of advanced support structure with micropiles of bamboo, the usability of new environmentally friendly building material, and the accessibility of the new pile laying method. This would offer the new idea in the shallow foundation support structure,

accelerate the use of scientific achievement in practical engineering, and save building materials effectively, thereby protecting the environment.

In recent years, scholars have carried out several studies on the foundation pit supports in soft soil areas. Dai et al. [1, 2] analyzed the bamboo prevention system with a three-dimensional (3D) nonlinear numerical method. The results indicate that bamboo piles with high bending strength can effectively resist stresses from outer parts of the foundation as well as external loads. The pile displacement was small, whereas the lateral and the vertical displacement were obtained to be in a reasonable range. The preventive effect was better than that of the C30 concrete piles under the same conditions. It, therefore, shows the practicability of the prevention system of single-row bamboo piles in soft soil shallow foundation pits. With the gradual increase in external loads, the single-row pile could not satisfy the prevention requirement. Although double-row piles can resist more external loads and maintain the stability of foundation pits, their preventive effect increases subtly. Deng et al. [3] conducted an indoor test on micropiles, and obtained results that are in good agreement with the infinite analysis results reported by Dai et al. [1, 2]. In the study, a new prevention method, combined with existing theories, was used in the foundation excavation and design of a park in Wuhan China. The new method combines the method of decreasing the inclination of earth slope and the prevention structure of single-row piles. The technology was ascertained to be able to decrease the total engineering cost by approximately 40%. The feasibility and economic effect of bamboo micropiles in soft soil foundation pits have been proved in engineering. Currently, research on bamboo micropiles is limited; most studies were conducted on the microstructure of bamboo. The application of bamboo in soft soil foundation pits is also limited, but its research and application have further spaces to be found.

In summary, bamboo sticks integrated with dentate row piles are used in foundation pits due to their environmental friendliness. The combination outmatches the traditional and single-pile laying methods. Model tests were conducted to verify the feasibility and stability of the dentate bamboo pile support for shallow foundation pits in soft soil. The method can compensate for the deficiency in soft soil foundation pits, avert the issue of underprevention or overprevention due to unreasonable test projects, optimize building materials, alleviate the shortcomings of building materials, and reduce air pollution. The obtained results provide positive effects and reference for the extended applications of bamboo piles and the innovation of support forms in shallow foundation pits [4, 5]. In the future, bamboo dentate row piles would not be confined in shallow foundation pits; rather, the complex bamboo support method would be used in ultradeep foundation engineering with complex engineering conditions.

2. Analysis of Foundation Pit Stability

In practice, the analysis of the foundation pit involves the analysis of the vertical slope with the support structures. The most frequently used methods of analysis are the Swedish slice method, Bishop method, and simplified Bishop method. In this study, the Swedish slice method is used to calculate the total stress. The sketch calculation map is shown in Figure 1.

The slice is analyzed as shown in Figure 1. The normal stress σ_i is expressed as follows:

$$\sigma_i = \frac{N_i}{l_i} = \left(\Delta G_i + qb_i\right)\frac{\cos\beta_i}{l_i}. \tag{1}$$

The shear stress in arc is given as follows:

$$\tau_i = \sigma_i \tan\varphi_i + c_i. \tag{2}$$

Sliding force is given as follows:

$$T_i = \left(\Delta G_i + qb_i\right)\sin\beta_i. \tag{3}$$

Sliding moment is given as follows:

$$M_s = R\sum T_i = R\sum\left(\Delta G_i + qb_i\right)\sin\beta_i. \tag{4}$$

Antisliding moment is given as follows:

$$\begin{aligned} M_r &= R\sum \tau_i l_i = R\sum\left(\sigma_i \tan\varphi_i + c_i\right)l_i \\ &= R\sum\left(\left(\Delta G_i + qb_i\right)\cos\beta_i \tan\varphi_i + c_i l_i\right). \end{aligned} \tag{5}$$

According to the force equilibrium equation, the total moment induced by each slice is zero. The factor of safety, K_{sj}, is calculated as follows:

$$K_{sj} = \frac{M_r}{M_s} = \frac{\sum c_i l_i + \sum\left(qb_i + \Delta G_i\right)\cos\beta_i \tan\varphi_i}{\sum\left(qb_i + \Delta G_i\right)\sin\beta_i}. \tag{6}$$

In the above equations, q is the external load on the earth's surface, and ΔG_i is the slice weight. φ_i, c_i, b_i, l_i, and β_i are the internal friction angle, cohesion, width of the slice, length of the slice, and the angle between the tangential and horizontal directions of the slice, respectively.

The Swedish slice method uses different radii and centers of the potential failure circle surfaces to determine the minimum factor of safety as expressed in equation (7). With this, the stability of the foundation pit can be determined.

$$K_s = \min\{K_{s1}, K_{s2}, K_{s3}, \ldots, K_{si}, \ldots\}. \tag{7}$$

The minimum factor of safety, K_s, is calculated by limit element analysis and the curve fitting method. K_s must be greater than 1.35 when the safety level is 1. The foundation pit stability is satisfied by the calculated result.

2.1. Calculation of Overturning Stability. Due to the narrow foundation pit area, excavation methods in which large area of the earth is excavated at the same time cannot be used. Building foundations are usually shallow, about 4–6 m. According to the demands of Technical Specification for Retaining and Protecting of Building Foundation Excavation (JGJ 120-2012), the embedded depth of pile should not be less than 0.4 times the excavation depth; otherwise, the stability of foundation pit would be influenced. Therefore, the embedded depth must be calculated. The excavation and embedded depths of indoor model tests are 0.4 m and 0.2 m, respectively. By contrast, in practice, they are 4 m and 2 m,

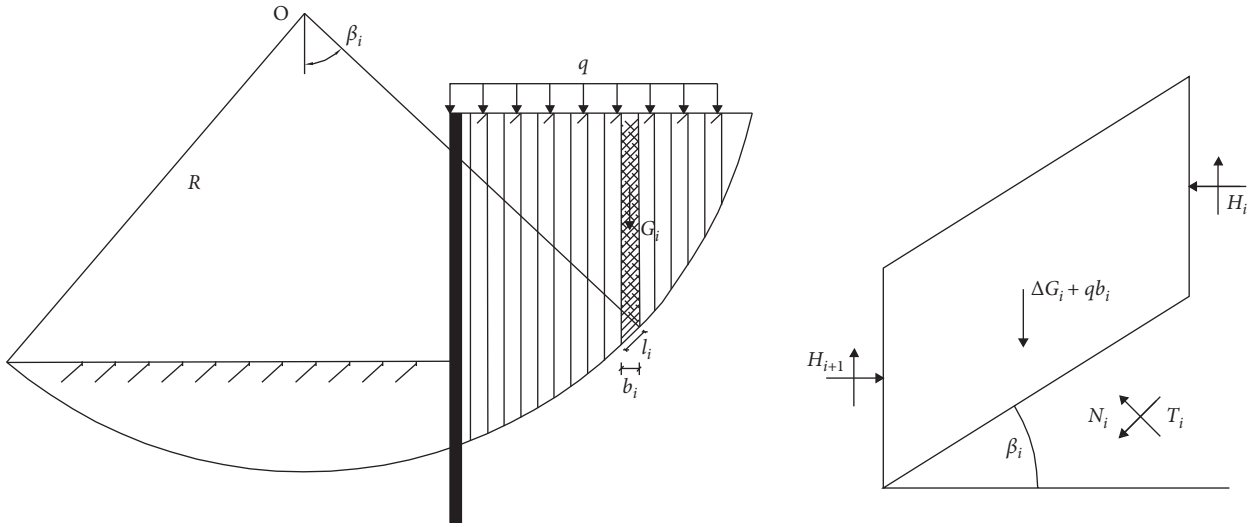

Figure 1: Analysis and calculation of overall stability of foundation pit.

respectively, according to the similarity ratio 1 : 10. A bamboo micropile support structure is used in this study. A theoretical embedded depth of piles, l_d, of 2 m and an additional load above ground q of 20 kPa are used. The distribution of the earth pressure is shown in Figure 2. In this study, the effect of underwater is not considered; however, the single layer earth is considered. The basic parameters of earth are listed in Table 1.

Active earth pressure is as follows:

$$M = \mathrm{EI}\frac{(\varepsilon_- + \varepsilon_+)}{h}, \qquad K_a = \tan^2\left(45^\circ - \frac{\varphi}{2}\right). \tag{8}$$

Passive earth pressure is as follows:

$$\sigma_p = \gamma z K_p + 2C\sqrt{K_p}, \qquad K_p = \tan^2\left(45^\circ + \frac{\varphi}{2}\right). \tag{9}$$

Calculation of stability is as follows:

$$K_q = \frac{M_p}{M_a} = \frac{E_p h_p}{E_a h_a} = \frac{181.10 \times 0.85}{77.06 \times 1.48} = 1.35 \geq K_e. \tag{10}$$

When the security grade is level 1, K_q is greater or equal to 1.25. Hence, the embedded depth of micropiles satisfies the minimum requirement for stability, and an embedded depth of 2 m can therefore be used.

3. Test Project

3.1. Similarity Scale Relation. According to the three similarity theorems, the similarity relation between the prototype and the experimental model can be obtained by the physical, geometric, and equilibrium equations and the boundary conditions. In general, the similarity scale of a dimensionless physical quantity is 1 and that of different

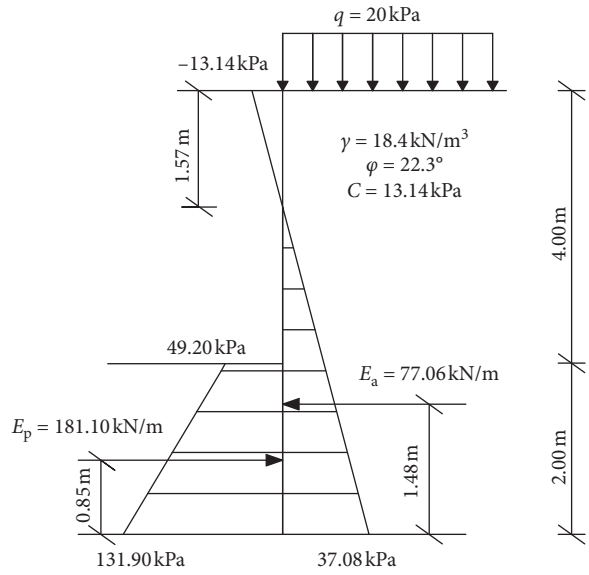

Figure 2: Distribution of earth pressure.

physical quantities with the same dimensions are the same. Considering the operability of each procedure in the model test, the geometric similarity ratio of the model test is 1 : 10. Table 2 lists the model-prototype ratios of each physical quantity.

It can be observed from Table 2 that the unit weight of the bamboo pile is 10 times that of the prototype; however, satisfying the test conditions are difficult. Since the main function of the bamboo piles is to withstand the horizontal soil pressure and the lateral deformation, the unit weight of the pile has little effect on the test results; hence, the similarity ratio can be reduced. Similarity constants of the geometry, unit weight, and strain are dependent on many similarity constants deduced from the similarity theory. Therefore, each physical and mechanical constant must satisfy the test requirement [4, 6]. To design a big scale model test, the scale of the experimental model and the prototype

Table 1: Basic earth parameter.

Earth	Density	Cohesion	Internal friction angle/limit	Volumetric modulus	Shear modulus	Poisson ration
Silty clay	18.4 kN/m^3	13.14 kPa	22.3	5.62*e*6 MPa	1.94*e*6 MPa	0.35

Table 2: Similarity relation of physical quantities.

Physical quantity	Dimension	Model/ prototype	Similarity coefficient	Physical quantity	Dimension	Model/ prototype	Similarity coefficient
Length	L	$1/N$	1/10	Stress	$ML^{-1}T^{-2}$	1/1	1/10
Area	L^2	$1/N^2$	1/100	Strain	1	1/1	1
Density	ML^{-3}	1/1	1	Displacement	L	$1/N$	1/10
Unit weight	$ML^{-2}T^{-2}$	$N/1$	10	Distribution force	$ML^{-1}T^{-2}$	1/1	1

should be 1 : 10. The similarity scale relations for other constants are shown in Table 3.

3.2. Experiment Design

3.2.1. Experiment Material

(1) Foundation Pit Material. The earth in the model box is made of silty clay as a single medium. The basic earth parameters are listed in Table 1. The earth backfill in complex geological conditions and the effect of underwater in foundation pits were not considered because of the shallow depth of the foundation pits. The original excavation stratum was simulated by artificial layering and tamping of the clay. The number of tamping for each layer needs to meet the design requirements ($T \geq 120$), and the compaction coefficient required for the test should also be fulfilled ($\lambda_c \geq 0.9$). After the completion of the continuous compaction of layers, the earth was allowed to rest for 72 hours. Subsequent work could be done sufficiently after the earth's compaction. During the filling process, on-site sampling was conducted to test the unit weight and water content. After the actual compaction, the earth unit weight and the water content were 18.4 kN/m^3 and 22.3%, respectively.

(2) Bamboo Micropile. Smooth and slim bamboos, devoid of molds, were selected for piles. Those having diameters 20–30 mm and length 0.6 m were selected, in accordance with the engineering and experimental requirements. The selected piles were numbered from 1 to 14 accordingly, as shown in Figure 3. Two strain gauges were attached to both sides of the bamboo piles as shown in Figure 4. The regularity of the lateral bending characteristics of the bamboo was simultaneously studied by the test of a simple reinforced concrete beam in the external load. The measured elastic modulus of bamboo was approximately 15 GPa.

3.2.2. Foundation Pit Model.

The size of the foundation pit was 1.20 m × 0.8 m × 0.4 m. The 14 piles were arranged on the short sides of the foundation pit: parallel piles on one side (pile spacing of 0.12 m) and the dentate piles on the other side (the same pile spacing). The outermost side pile was placed 0.0878 m away from the long sidewall, and the innermost side pile 0.06 m away from the short sidewall. On the long sides of the foundation pit, seven bamboo piles were arranged on each side and connected together by a crown beam to enhance their overall stiffness. Due to the asymmetric loading method, the load on one short side has little effect on the other short side such that its deformation could be ignored. Therefore, two types of piles were arranged in the same foundation pit, as shown in Figure 5.

Table 3: Constants' similarity relation in the model test.

Physical quantity	Relation	Similarity ratio
Physical dimension L	C_L	10
Unit weight γ	C_γ	1
Strain ε	C_ε	1
Displacement δ	$C_\delta = C_L + C_\varepsilon$	10
Stress σ	$C_\sigma = C_L + C_\delta$	10

Figure 3: Bamboo micropile.

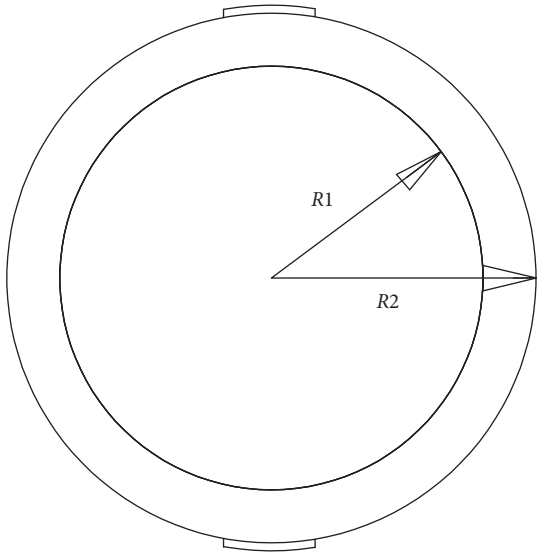

Figure 4: Strain gauge arrangement.

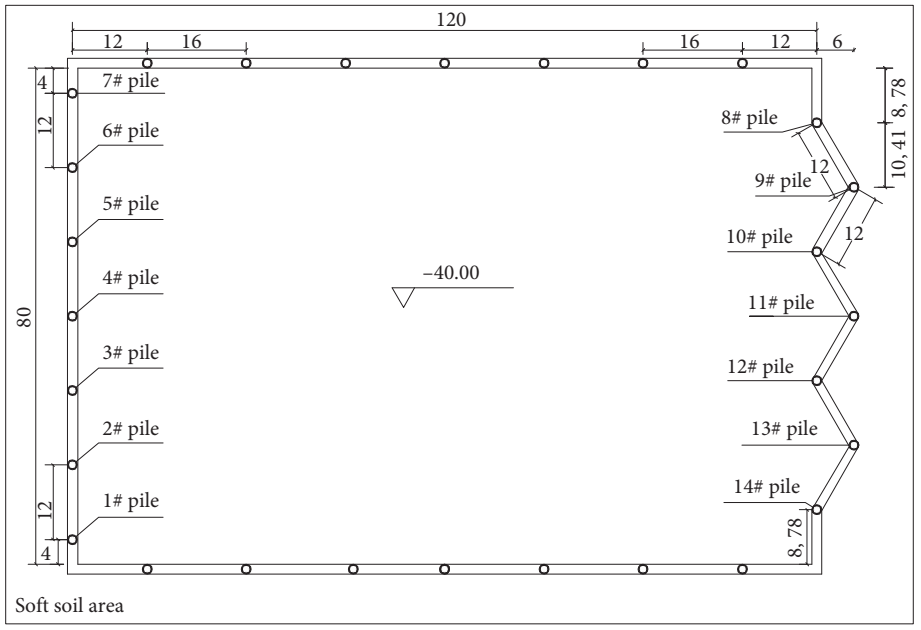

(a)

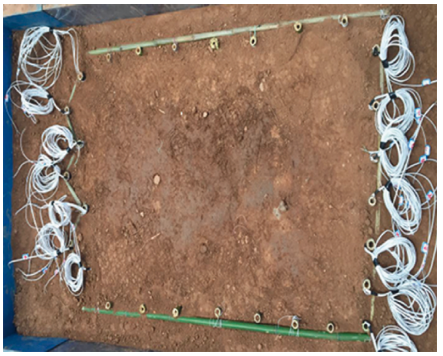

(b)

(c)

Figure 5: Foundation pit model. (a) Foundation pit plan. (b) Before excavation. (c) After excavation.

3.2.3. Measuring System

(1) Displacement Measurement. The settlement of the pile-soil system and the displacement of the top part of the piles were measured by the TST-50 strain displacement gauges and the dial gauges. The displacement gauges were arranged at 0.18 m away from the sidewall of the short side of the foundation pit, with a spacing of 0.05 m. The dial gauges, on the other hand, were placed at the top of the piles numbered 2, 4, 6, 8, 10, and 12. The data were collected in 30 min intervals.

(2) Deformation Measurement. A BX120-1AA (1 mm × 1 mm) of strain gauge of base size, 7.3 mm × 4.1 mm, was used to measure the strain of the piles. A TST3826E static strain test analysis system, with up to 1 $\mu\varepsilon$ resolution, was used for the data acquisition. The strain gauges were arranged symmetrically along the pile at depths of 0.1, 0.3, and 0.5 m. For piles 4 and 10, the strain gauges were placed at 0.1 m interval along the pile bodies to collect and analyze the stress changes in the bamboo piles during the excavation processes. The data were collected every 5 min. The detailed layout is shown in Figure 6.

(3) Earth Pressure. The earth pressure was measured using a TXR-2030 microearth pressure gauge with its resolution less than 0.05% F•S and a measurement range of 0–0.8 MPa. When the soil was filled layer after layer, the pressure gauges were pre-embedded in the vicinity of the 4, 6, 10, and 11 piles, according to the excavation depth of the foundation pit and the position of the bamboo piles. They were arranged at 0.1 m intervals along the length of the bamboo pile. The data were collected every 30 min.

3.2.4. Loading Scheme. Prior to excavation, a certain amount of load should be applied until the foundation pit is completed. The loading stage was divided into three processes. Each stage of load was 3.28 kPa. All loads were applied by the mass-block-stacking method. After each loading stage, the data were recorded when it was stable, after which the next loading stage commenced. The loading sketch map is shown in Figure 7.

4. Results and Discussion

4.1. Displacement and Deformation. According to the data collected by the displacement gauges on the short sides, the surface settlement of the foundation pits of the straight row and that of the dentate piles are small during the excavation process. It increased gradually with an increase in the load. The maximum settlement of the straight-row pile was 2.35 mm, whereas that of the dentate pile was 1.88 mm, both of which are small and within a reasonable range. The new pile laying method was observed to effectively restrain vertical displacement of the foundation and transmit diversional stress.

From the top part of pile displacement curves, shown in Figure 8, it can be seen that the top part of piles 4 and 10 have the largest horizontal displacement in each short side: 2.14 mm and 1.65 mm, respectively. The horizontal displacement of the outer pile also showed a slight difference. In the actual project, the top part of the pile should be restrained to control the horizontal displacements, so as to ensure the safety of the foundation pit. In the loading process, the horizontal displacement of the top part of straight-row piles increased greatly. In the second loading stage, part of the soil mass at the front edge of the straight-row pile top fell off, and the sidewall of the foundation pit was raised slightly. This indicates that the slope supported by the straight-row piles has a tendency of sliding to the foundation pit. With increase in loading, the damage gradually developed from the shallow layer to the deeper layer. When it exceeded the antisliding force of the slope, the soil sheared and slipped as well as the slope slid. There was no apparent gap in the sidewall and fallen soil block in the foundation with dentate row piles. The change in the regularity of the horizontal displacement in the top part of pile was apparent, and the horizontal displacement value of dentate row pile was less than the value of the single-row pile. This could be attributed to the fact that bamboo piles were the main structure that resisted the load, which were far from the sidewall of the foundation pits, to carry most of the loads, and effectively resisted the soil stress with high compaction and bending resistant strength in the load delivery. Hence, there was little horizontal displacement of pile in the inner row. In conclusion, we infer that the dentate piles are superior to the straight-row piles in controlling horizontal and vertical deformations of foundation pits. Therefore, it can restrain deformations of foundation pits and effectively ensure its stability.

4.2. Pile Earth Pressure State. The piles in the middle area are less affected by the boundary conditions. Therefore, the 4, 10, and 11 piles were taken as the case study to explore the change of earth pressure in the excavation and loading processes.

4.2.1. Change of Earth Pressure Behind Piles during Excavation. As can be seen from the measured earth pressure distribution curves of pile 10 (Figure 9), above the excavation surface, the earth's pressure decreased gradually. However, its total change was significant with the increase in the excavation depth, whereas the change in the earth pressure was small below the excavation surface. These indicate that the failure of soil mainly occurs above the excavation surface, extends to the surface below the bottom of the foundation pit, and gradually develops to the deep layer. When the excavation depth was 0.25 m, the earth pressure became zero. It was observed that as the excavation progressed, the earth pressure gradually transited from a static state to an active state, which could lead to the separation of the pile from the soil. Therefore, the earth pressure of some measured points suddenly became zero. The process of the foundation pit excavation changed the stress distribution of the soil behind the piles. As the excavation depth increases, the stress concentration point gradually shifts down [5].

4.2.2. Analysis of the Change of Earth Pressure Behind Piles in the Loading Stage. From the change in the earth pressure, behind the piles, during the loading phase shown in Figure 10, it can be observed that the change in the earth

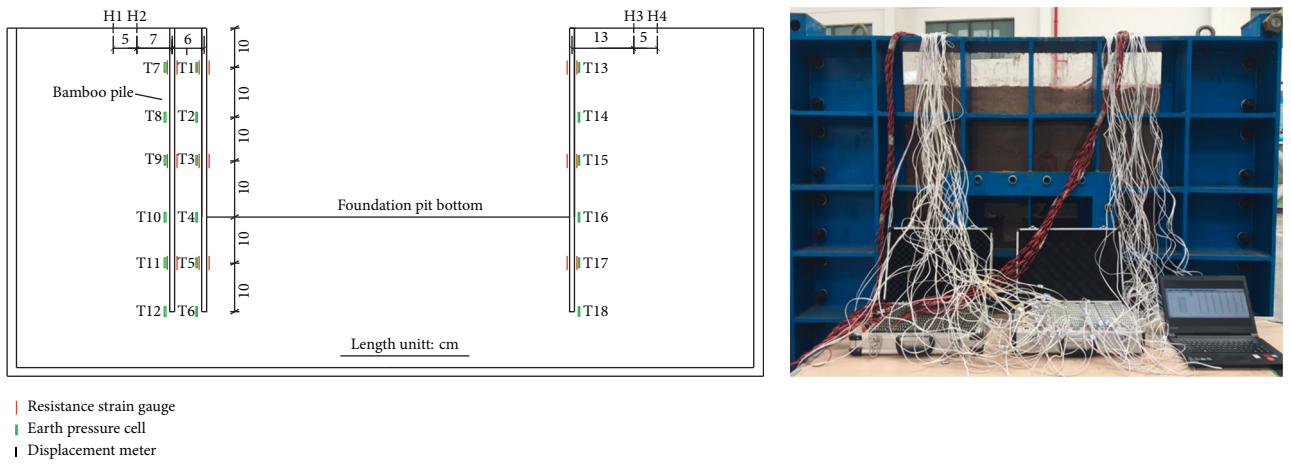

Figure 6: Measurement layout scheme and data acquisition. (a) Monitoring point arrangement. (b) Data collection.

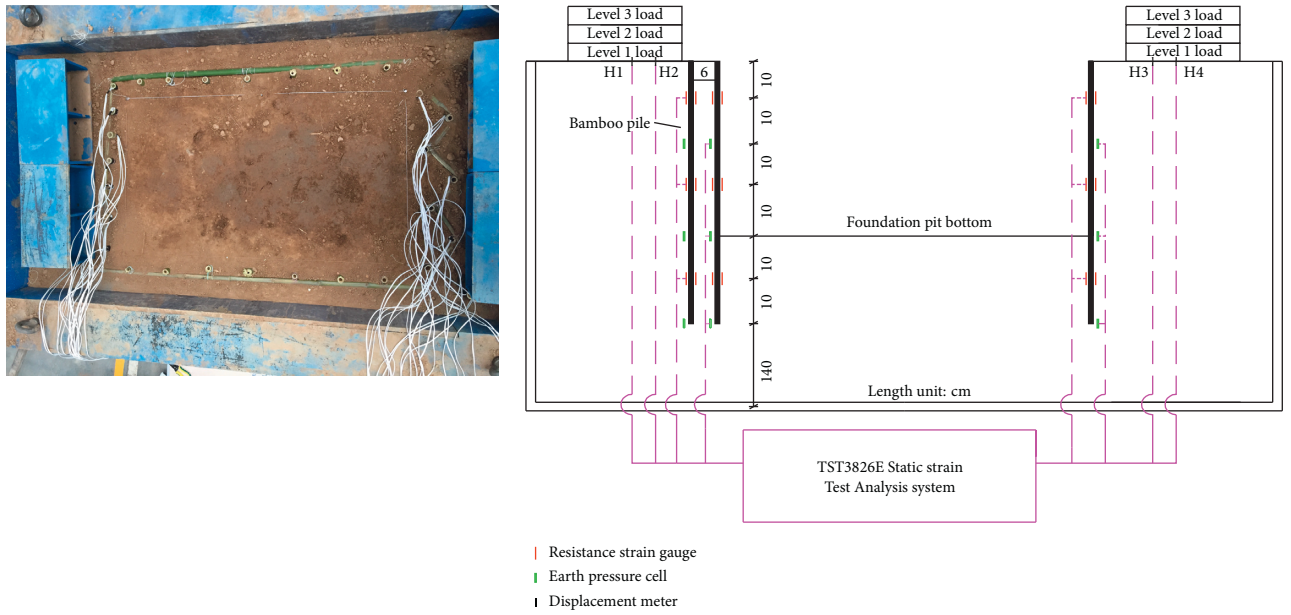

Figure 7: Mass loading. (a) Preloading in excavation stage, and (b) servo hydraulic control system.

pressure behind piles of the straight-row piles and that of the dentate piles were basically the same. With the increase in load, the earth pressure increased gradually. Above the foundation excavation surface, the pressure increased rapidly, whereas little fluctuation was observed below the excavation surface. This is attributed to the fact that the top and medium parts of the pile resisted most of the load; hence, the external load gradually decreased in the load delivery from the top of the pile to the bottom. Meanwhile, it was found that the increment in the earth pressure of superstructures in the preliminary loading process was larger than that in the next loading stage. The stress mechanism of soil was analyzed. Soil pores were gradually compacted firmly. In the stress transmitting process, the stress increased rapidly during the initial loading stage, but steadily in the later loading phase. For pile 4, the earth pressure changed irregularly in the 0.3 m area of the middle part. When the load reached 13.12 kPa, the earth pressure at the bottom of the foundation pit increased suddenly, indicating that the damage in the foundation pit appears in the middle and bottom parts. However, the overall trend of the dentate pile area was stable, and there was no uplift or falling off of the soil layer on the surface of the foundation pit. It, therefore, indicates that shear failure often shows in the medium and bottom of foundation pits with the single-row pile, but dentate bamboo piles resist part of the load with the influence in the stress delivery and distribution; most of the loads are delivered to the soil around the pile. The failure

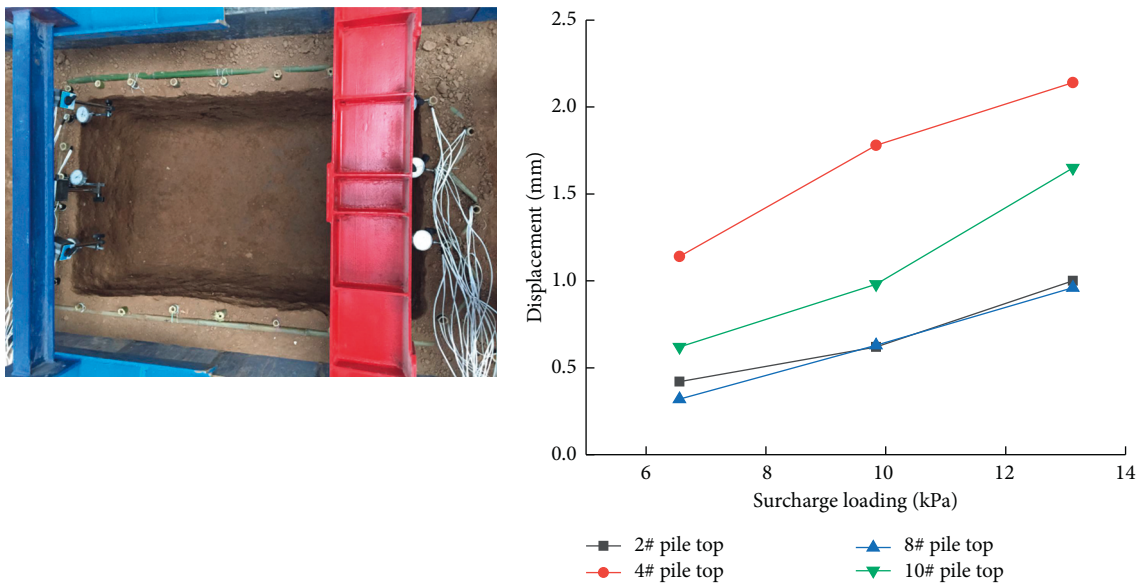

Figure 8: Column top displacement measurement. (a) Dial indicator layout. (b) Pile top displacement curves.

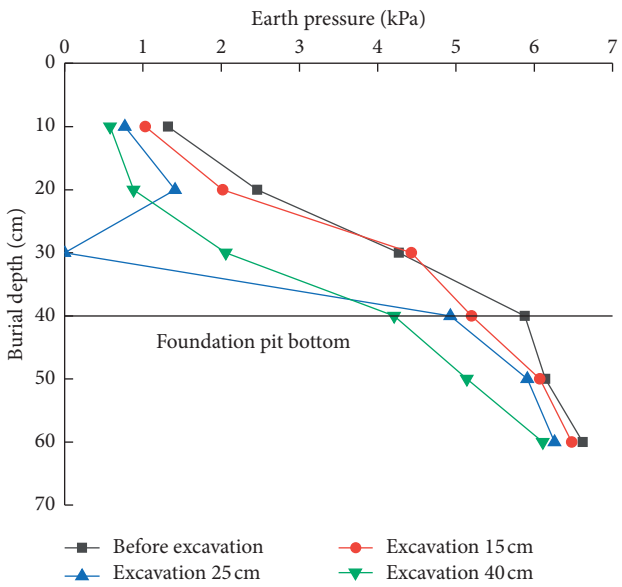

Figure 9: Earth pressure distribution curves behind piles in excavation.

section of the dentate pile showed in the medium and bottom of foundation pits with more load. Therefore, it is necessary to reinforce the soil layer in the middle and lower parts of the foundation pits to ensure stability and safety.

4.3. Characteristics of the Pile Stress

4.3.1. Analysis of the Moment of Piles during Excavation. The bending moments at each point of the micropile were calculated by applying the bending theory in the Machine of Materials and the strain gauge on both sides of the pile. The equation for the calculation is as follows:

$$M = \frac{\mathrm{EI}\left(\varepsilon_{-} + \varepsilon_{+}\right)}{h}, \tag{11}$$

where M is the bending moment of the pile body, EI is the bending stiffness of the micropile, ε_{-} and ε_{+} are the tensile and compressive strains of each measuring point, respectively, and h is 0.022 m, which is the spacing between the tensile and compressive strain points on the same cross-section. The results are tabulated in Table 4.

It can be seen from Figure 11 that the bending moment of single-row piles varies greatly in the excavation process, and the bend in the pile body is similar to that of a loaded cantilever beam. The bending moments of the dentate piles are, however, relatively stable. With the increase in the excavation depth, the bending moment of each point increases gradually and its total change becomes high. When the excavation depth reaches the design depth of 0.4 m, the maximum positive bending moment of the pile 4 and the pile 10 would be about 626.16 N·m and 548.6 N·m, respectively, whereas the maximum negative bending moments would be about −686.31 N·m and −596.34 N·m, respectively. The above analysis shows that in the process of excavation, the traditional single-row piles resist lateral and upper loads; hence, each of the piles is under an intensive stress condition. Therefore, the capacity of the foundation pit system decreases. However, in the case of the dentate pile structure, the delivery path and the method of loading are considered, hence, the stress can be reduced, layer by layer, from the top part of the pile to the lower part. Dentate piles can also utilize its special space to deliver and distribute stresses reasonably. The new foundation system can withstand more loads. In the single-row piles, there are higher shear forces and more bending moment fluctuations. Relative experimental phenomenon and the

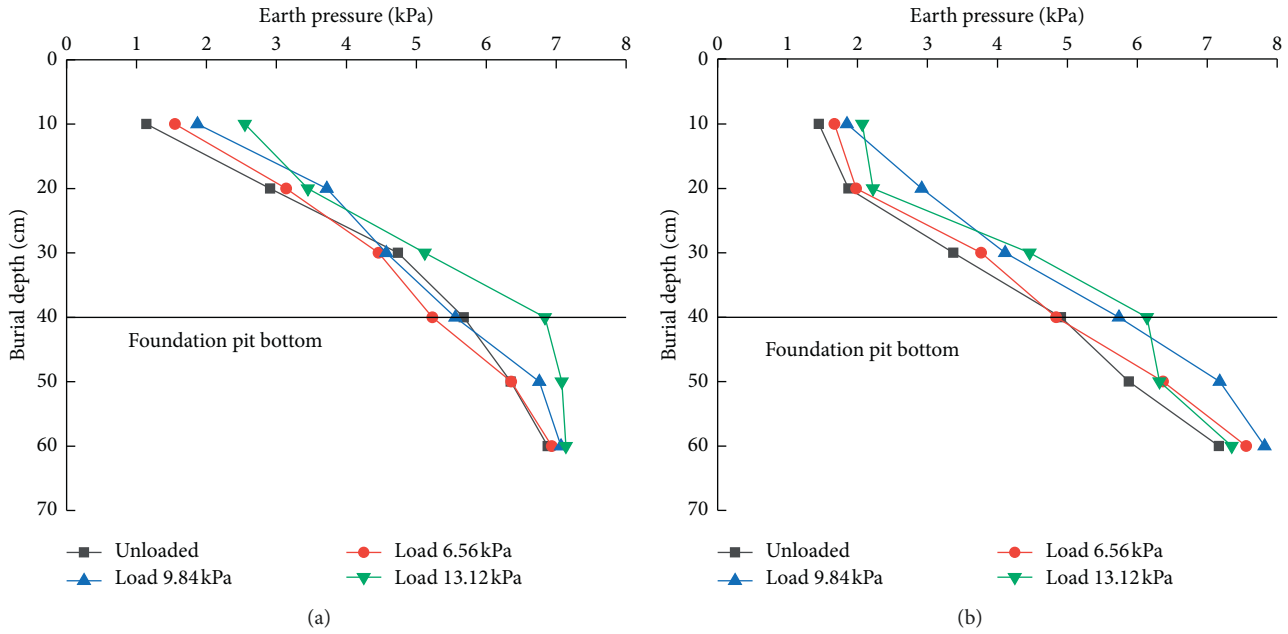

Figure 10: Earth pressure distribution curves behind piles in the loading stage. (a) Earth pressure of pile 4. (b) Earth pressure of pile 11.

Table 4: Calculation of pile bending moment.

Pile number	Depth (cm)	d (mm)	D (mm)	EI (N·m^2)	M (N·m) (15 cm)	M (N·m) (25 cm)	M (N·m) (40 cm)
4	10	16	22	124.17	115.81	149.47	186.45
	20	16	22	124.17	172.86	256.54	399.27
	30	16	22	124.17	−201.93	−433.1	626.16
	40	16	22	124.17	−246.93	−359.5	−686.31
	50	16	22	124.17	−40.36	−56.98	−125.98
	60	16	22	124.17	−68.21	−82.87	−154.43
10	10	16	22	124.17	59.31	89.03	148.73
	20	16	22	124.17	91.01	216.2	315.61
	30	16	22	124.17	142.03	234.48	548.6
	40	16	22	124.17	123.45	−391.5	−596.34
	50	16	22	124.17	23.6	−64.39	−113.48
	60	16	22	124.17	49.15	−70.8	−126.18

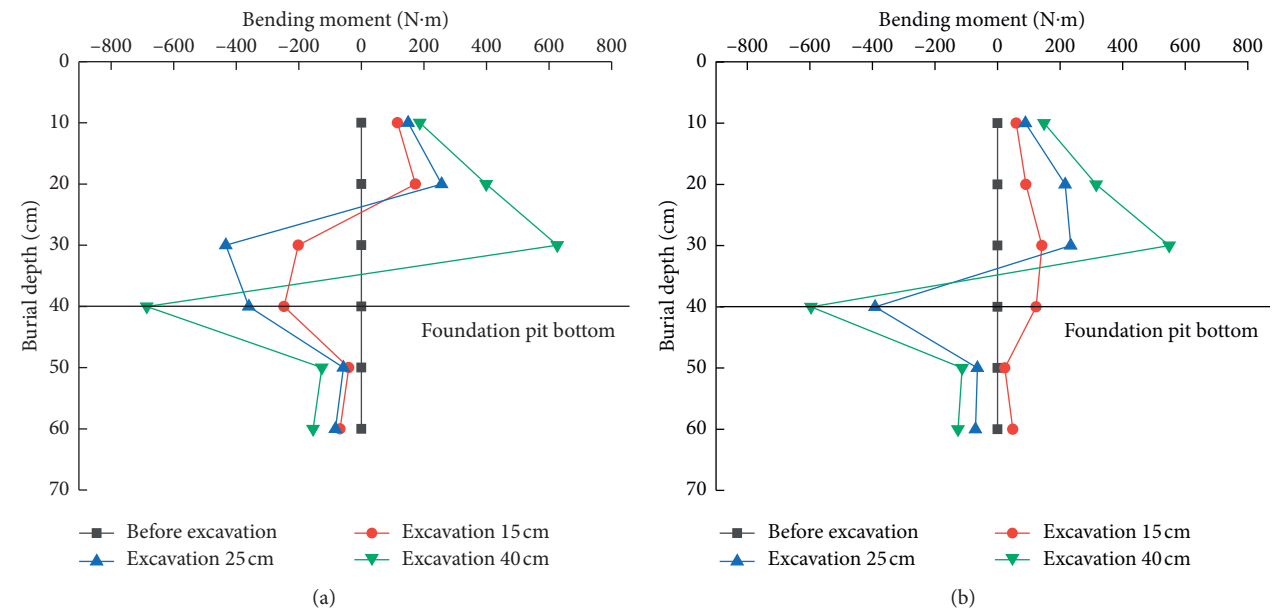

Figure 11: Moment curves of each pile body during excavation. (a) Pile 4. (b) Pile 10.

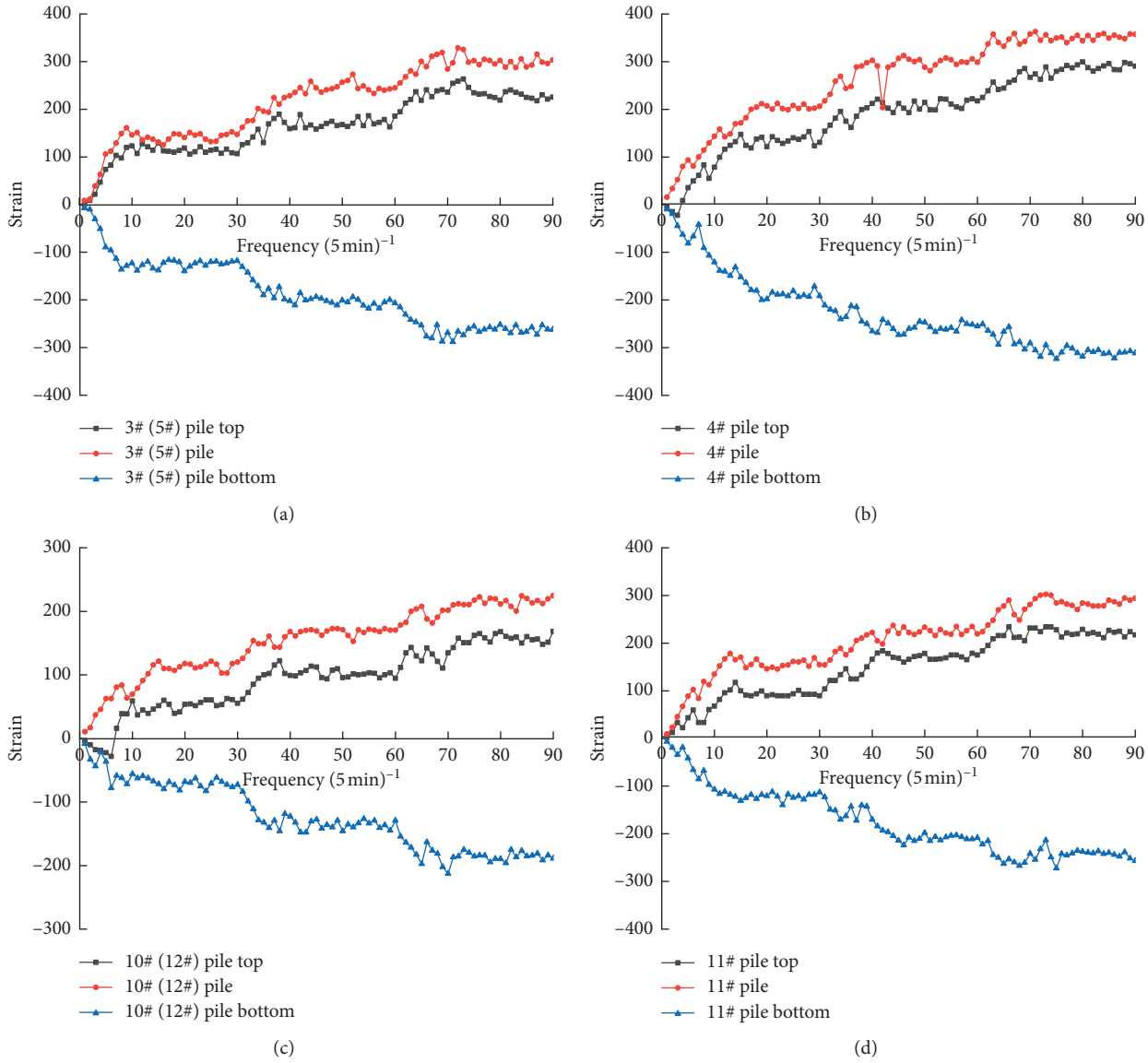

Figure 12: Pile strain time curves. (a) Pile 3. (b) Pile 4. (c) Pile 10. (d) Pile 11.

results prove the advantages of dentate piles compared to the single-row piles. Not only should the strength of piles be considered, but also the pile site and the stress delivery path should be inserted into the project to ensure the security, stability, and economic benefits of the support structures in foundation pits.

4.3.2. Pile Deformation during Loading. Considering the symmetrical structure and the load, piles 3, 4, 10, and 11 were chosen as the experimental piles and their experimental data were collected to picture the strain figure of piles.

According to the strain versus time curves of the two types of piles, shown in Figure 12, the strain of piles increases gradually with time. For the straight-row piles, the data were stable after approximately 1.5 h of each loading stage, and the deformation of piles were stable. However, for the dentate piles, the increase in strain stopped, about an hour after loading, which is consistent with the change in the earth pressure behind the pile. The top and middle parts of each pile were subjected to compressive strain (the pressure in front of the piles was assumed to be positive and the tension behind the pile to be negative). By contrast, the bottom part of the pile was subjected to tensile strain. Thus, under this condition, the reverse bending point of the pile was located at the middle and lower parts, between the depth of 0.3 and 0.5 m. The highest pile strain was observed in this area, and zero point occurred only once. In practice, this part should be reinforced with steel bars. For both types of piles, the pile strain in the middle part is higher than that at the top, which is in turn higher than that at the bottom. The maximum strain in the straight-row pile was recorded in the middle part pile 4 (358.93 $\mu\varepsilon$), whereas it was obtained in the inner side of pile 11 (302.04 $\mu\varepsilon$) in the case of the dentate piles. The reason is that the dentate piles are two

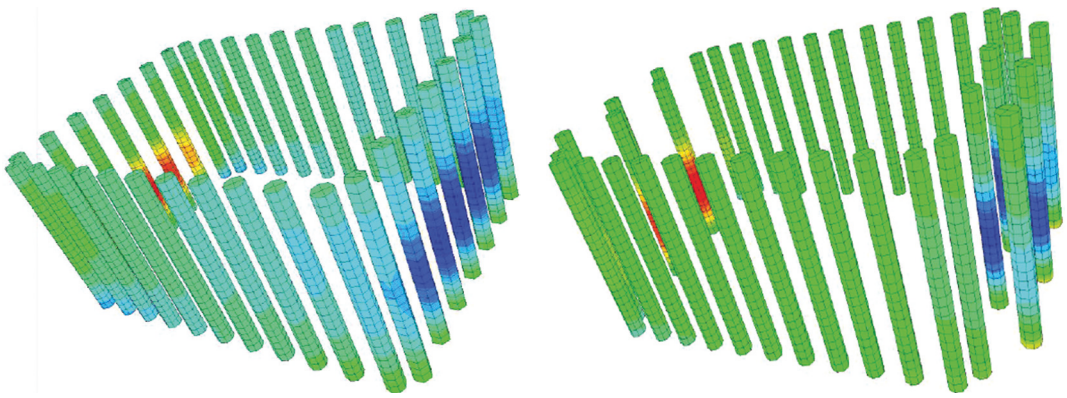

(a) (b)

Figure 13: Pile deformation cloud map. (a) Single-row pile. (b) New pile type.

rows of parallel asymmetric piles. Therefore, under external load and earth pressure, the outer row of piles bears the internal stress of the soil, improves the stress distribution, and delays the formation of the sliding surface. By contrast, the inner side row piles can bear more load. The pile-soil interaction reduces the stress level of the composite soil, improves the deformation performance, and is convenient for structural security and stability. The displacement nephogram of piles can be obtained by numerical simulations. As shown in Figure 13, the nephogram witnesses pile deformation regularity. The main performance shows little deformation, even distribution of the bending moment, and slight fluctuation of the data. According to the experimental data and the results, dentate piles are better than the traditional straight-row piles in terms of support and deformation resistance. Therefore, the new pile laying method is accessible.

5. Conclusions

In the excavation stage, the dentate piles can control the horizontal and vertical displacements better than the straight-row piles. They also form better constraints. The maximum strain of the dentate pile, the maximum pile top displacement, and the maximum positive bending moment of the pile body were obtained to be 302.04 $\mu\varepsilon$, 1.65 mm, and 548.6 N·m, respectively. Compared with the traditional straight-row piles, the support deformation and the lateral displacement of the dentate piles are smaller and are within the acceptable range, hence guaranteeing safety.

During the loading stage, the earth pressure on the straight-row piles above the bottom of the foundation pit fluctuated severely. However, the sidewall of the foundation pit was raised, and part of the soil mass on the top of the pile fell off. By contrast, there was a slight change in the earth pressure at the bottom of the foundation pit for both types of piles. With the increase in the load, the earth pressure of dentate piles increased linearly and slightly. In addition, no sidewall bulge or soil mass fall off occurred. Thus, dentate piles can resist greater earth pressure and external load than the straight-row piles.

In the excavation and loading stage, maximum deformation occurred at the middle part of the piles in the middle area of the short sides of the foundation pit, whereas the minimum deformation occurred in the lower part of the piles. Intermediate deformation was observed at the top part of the piles. Meanwhile, the upper and middle parts of the piles were subjected to compressive strain, whereas the lower part was under tensile strain. This shows that the reverse bending point of the pile is located in the middle and lower parts (30–50 cm). In practice, this part should be reinforced to ensure safety.

Foundation-pit support is a temporary project, so there is a need to minimize its production costs while ensuring safety. The use of bamboo materials instead of reinforced concrete not only ensures the stability of foundation pit at the excavating and supporting stages but also considerably reduces the project costs as well as the construction period. It reduces air and soil pollution caused by high-energy-consuming materials such as cement and steel, and conforms to the developing concept of environmentally friendly construction and eco-city. However, bamboo is vulnerable to moisture in a humid environment, which affects its strength. Therefore, the bamboo piles must be subjected to moisture-proof treatment so as to make them suitable for constructions in soft earth foundation pits with high water content or a long construction period. According to a series of tests, the dentate piles were found to support the shallow foundation pit in soft soil better than the traditional straight-row piles. Stresses and deformations are also less in the dentate piles. Thus, dentate piles are more effective in terms of support and are promising in the foundation-pit support for soft soil areas in the future.

Data Availability

The data used to support the findings of this study are included within the article.

Conflicts of Interest

The authors declare that they have no conflicts of interest.

Acknowledgments

The authors thank the workers, foremen, and safety coordinators of the main contractors for their participation. This work was supported by the National Natural Science Foundation of China (grant nos. 41672308 and 51878554).

References

[1] Z.-H. Dai, W.-D. Guo, G.-X. Zheng, Y. Ou, and Y.-J. Chen, "Moso bamboo soil-nailed wall and its 3D nonlinear numerical analysis," *International Journal of Geomechanics*, vol. 16, no. 5, Article ID 04016012, 2016.

[2] Z. H. Dai, Y. J. Chen, G. X. Zheng et al., "Numerical analysis on mechanism of bamboo soil nails and bamboo piles in rows for retaining deep foundation pit," in *Proceedings of the Tunneling and Underground Construction*, vol. 242, no. 2, pp. 720–730, Geotechnical Special Publication, Shanghai, China, May 2014.

[3] Y. S. Deng, H. Wang, M. Yang et al., "Model tests on shallow excavation support through bamboo micro-piles," *Rock and Soil Mechanics*, vol. 37, no. 2, pp. 294–300, 2016.

[4] D. Mitch, K. A. Harries, and B. Sharma, "Characterization of splitting behavior of bamboo culms," *Journal of Materials in Civil Engineering*, vol. 22, no. 11, pp. 1195–1199, 2010.

[5] M. J. Thompson and D. J. White, "Design of slop reinforcement with small diameter piles," in *Proceeding of the Advances in Earth Structures*, Shanghai, China, June 2006.

[6] J. K. Yan, Y. P. Yin, Y. M. Men et al., "Model test study of landslide reinforcement with micro-pile groups," *China Civil Engineering Journal*, vol. 44, no. 4, pp. 120–128, 2011.